B18 Chassis Design Report

Sachin DeYoung
UC Berkeley Formula SAE

Andrew Plewe, Adam Castiel, Max Lee, Raghav Jalan, Henry Cheung, Sarah Yue

June 20, 2018

Contents

1 Design

1.1 Torsional Stiffness

K_C = Chassis Stiffness

K_F = Front Suspension Stiffness

K_R = Rear Suspension Stiffness

W_F = Front Sprung Weight

W_R = Rear Sprung Weight

H_F = Front Sprung Center of Gravity Height

H_R = Rear Sprung Center of Gravity Height

$$LLTD = \frac{K_F * K_R * H_F * W_F + K_R * K_C * (H_F * W_F + H_R * W_R)}{(H_F * W_F + H_R * W_R) * (K_F * K_R + K_F * K_C + K_R * K_C)} \tag{1}$$

$$Sensitivity\, of\ K_F = \frac{K_F}{LLTD}\frac{\delta LLTD}{\delta K_F} \tag{2}$$

$$Sensitivity\, of\ K_R = \frac{K_R}{LLTD}\frac{\delta LLTD}{\delta K_R} \tag{3}$$

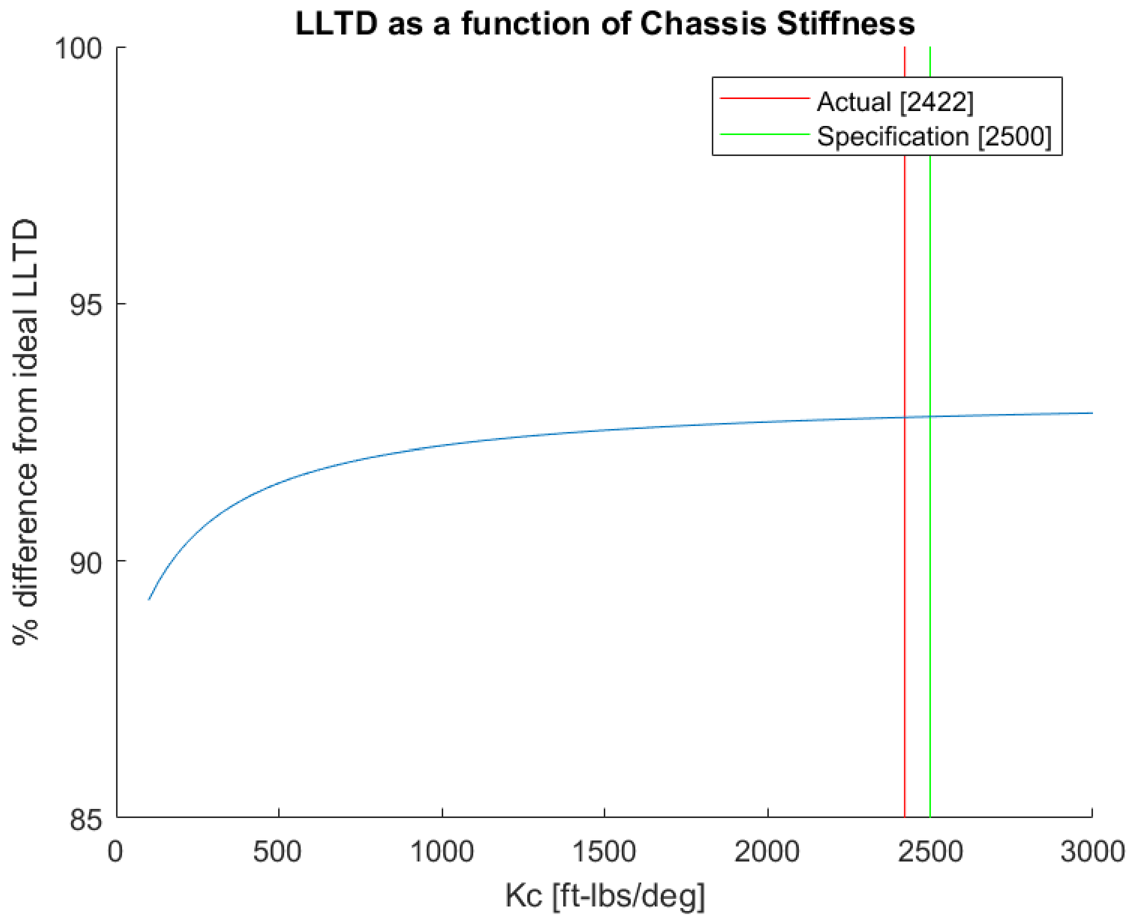

Figure 1: The difference in LLTD between a rigid chassis and a finite-stiffness chassis. This plot gives us confidence in assuming a rigid chassis in our tuning calculations.

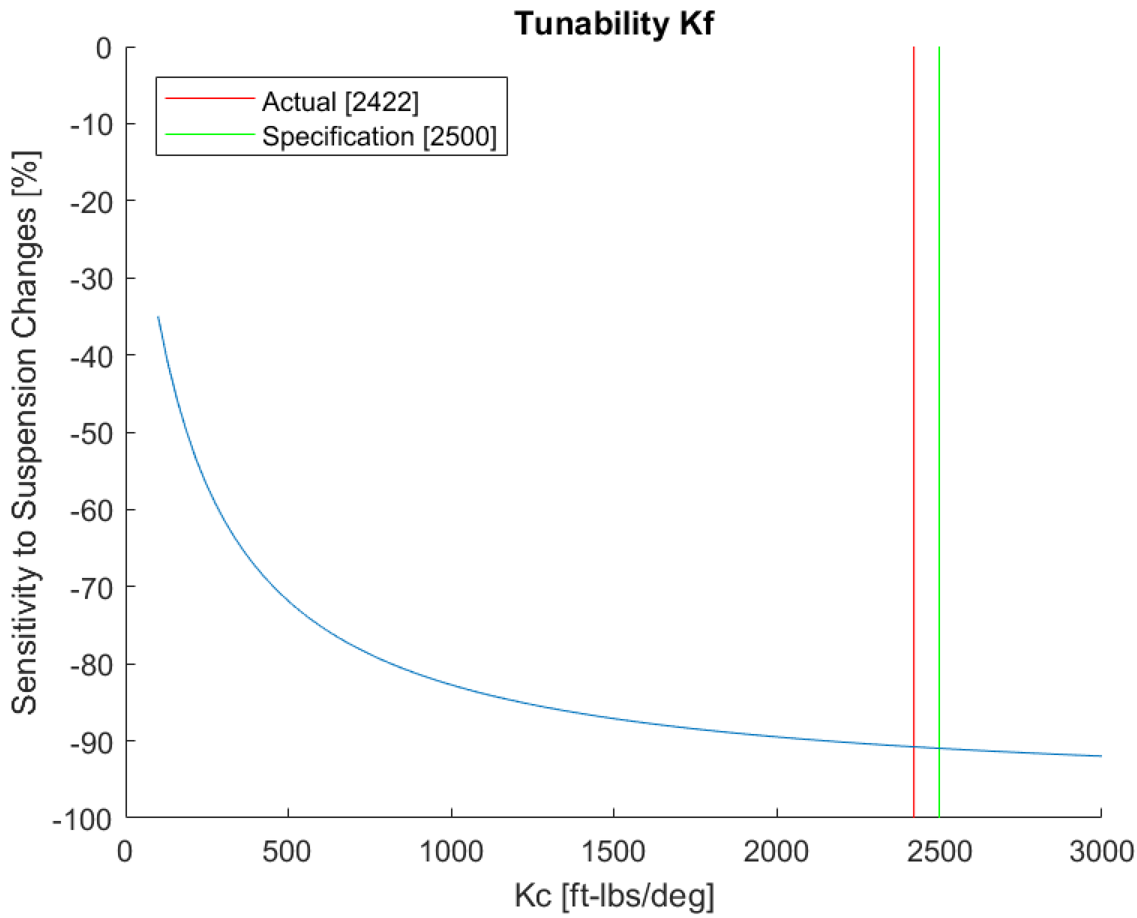

Figure 2: The effectiveness of one unit of change in the front suspension on the LLTD of the car. Our spec is at 90% effectiveness.

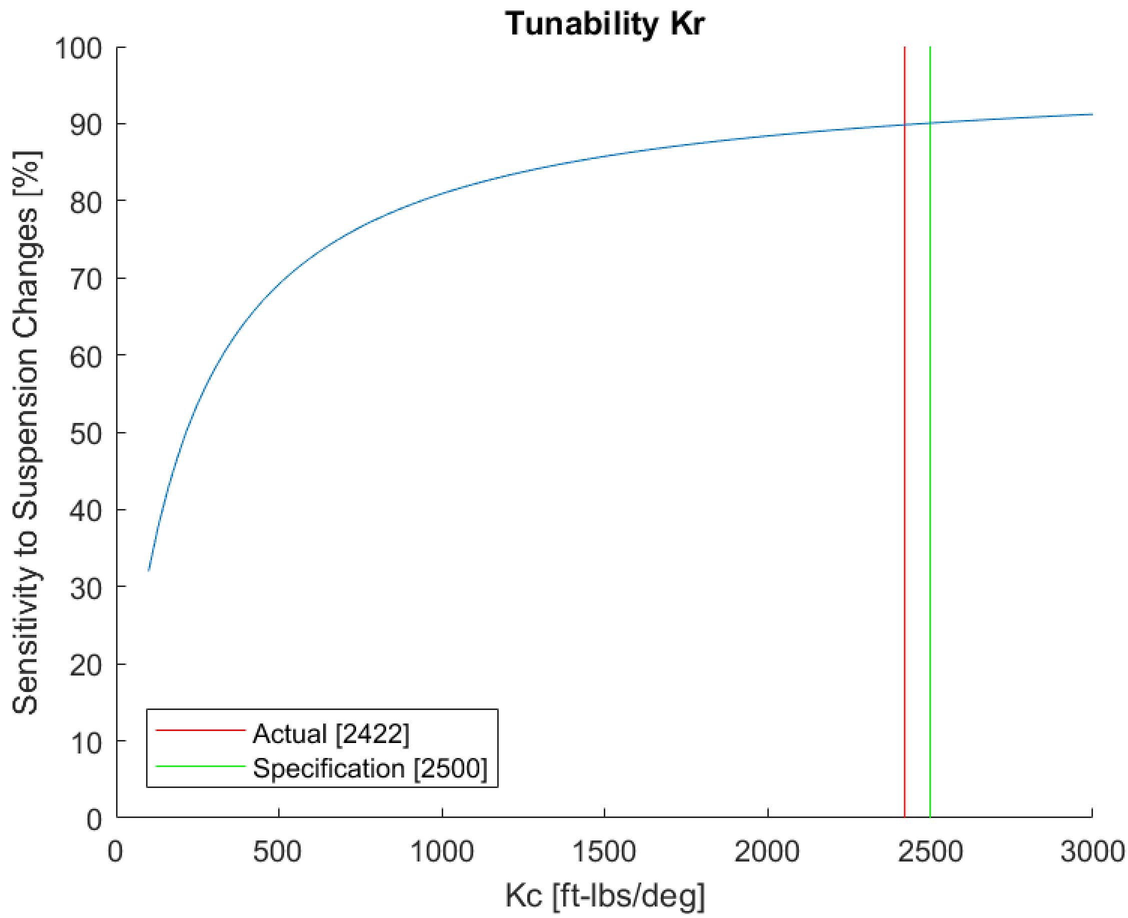

Figure 3: The effectiveness of one unit of change in the rear suspension on the LLTD of the car. Our spec is at 90% effectiveness.

1.1.1 FEA Setup

- We use a beam element based FEA in SolidWorks
- The suspension is included and modeled as rigid elements with realistic end conditions
- The system is constrained in 6 DoF, not overconstrained
- Forces are applied in opposite directions at the front uprights

1.1.2 Physical Test Setup

1.1.3 Results

1.2 Suspension Geometry

1.2.1 Goals

1. Feasibility of suspension points

2. Least weight possible

	Pullrod-Horizontal Shock	Dual Shock	Pullrod-Vertical Shock
Torsional Stiffness (ft-lbf/deg)	2800	2300	2500
Weight (lbs)	69.6	60.1	61.6
Stiffness to Mass Ratio	40	38.3	40.6
CGx (percent of total length)	53.6	58.0	56.5
MOI (lbs*in2)	249	222	235

The Front Hoop is green, and the Front Bulkhead is red. The suspension is in blue.

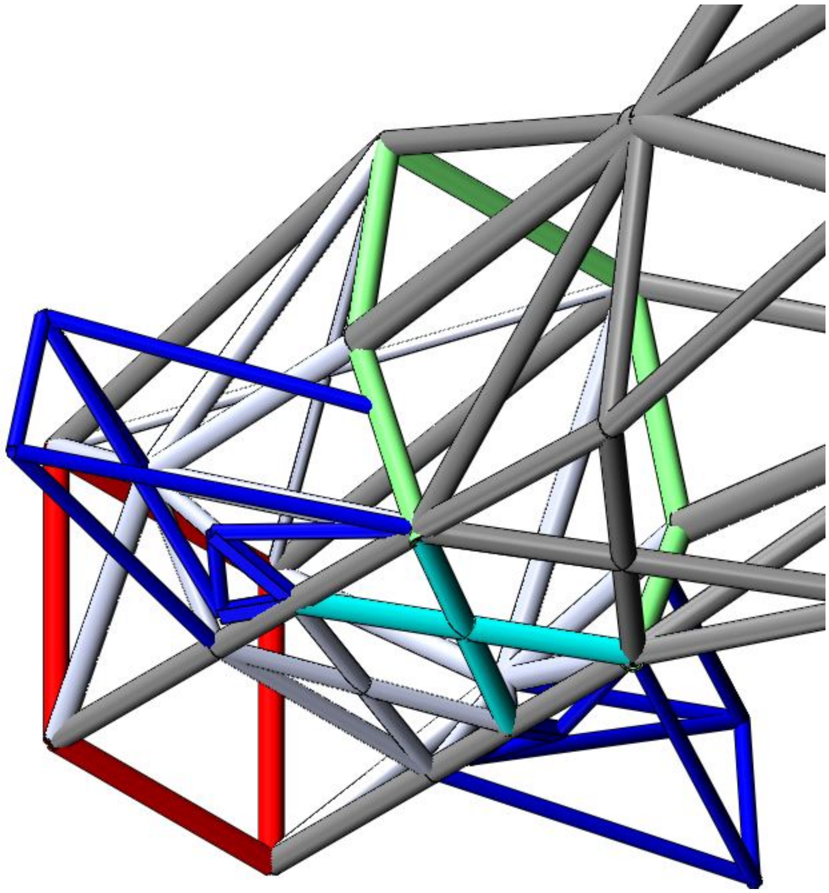

Figure 4: Horizontal-Shock Pullrod Design. The shock is triangulated into the base of the front hoop. The picture is taken from the lower left rear of the car.

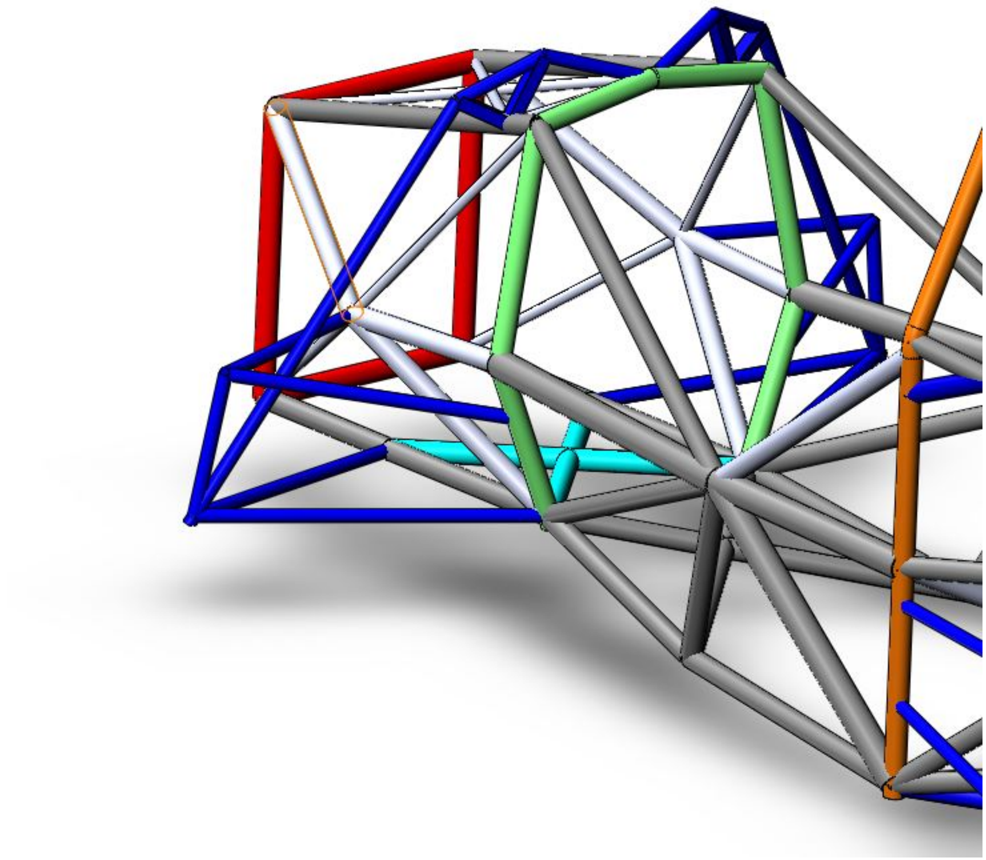

Figure 5: Over the Front Hoop Pushrod Design. The picture is taken from the upper left rear of the car.

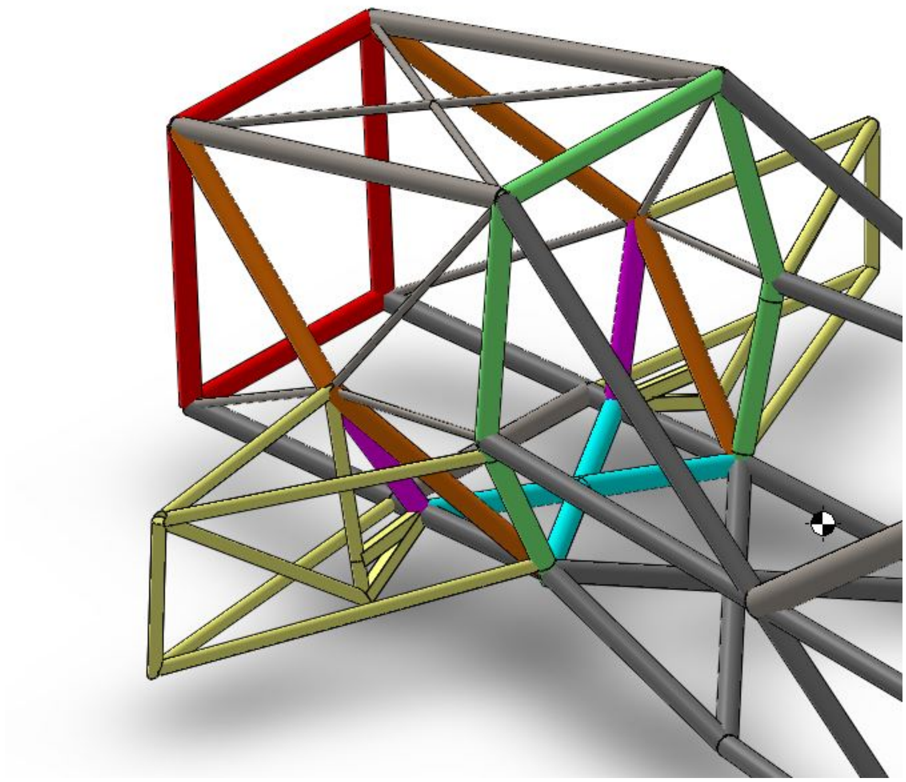

Figure 6: Vertical-Shock Pullrod Design. The picture is taken from the upper left rear of the car.

2 Suspension Compliance

2.1 Specification

Max compliance is 0.1 deg/G

2.2 Deflection Under 2.2G Braking

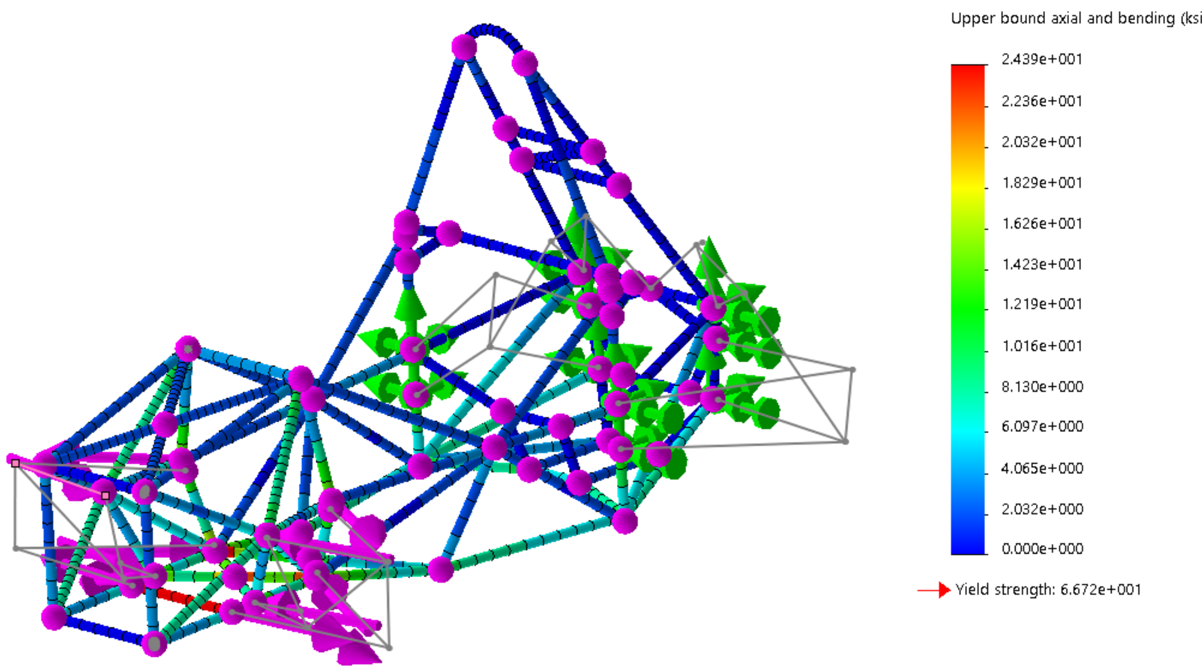

Figure 7: Stress on Front Points Under 2.2G Braking

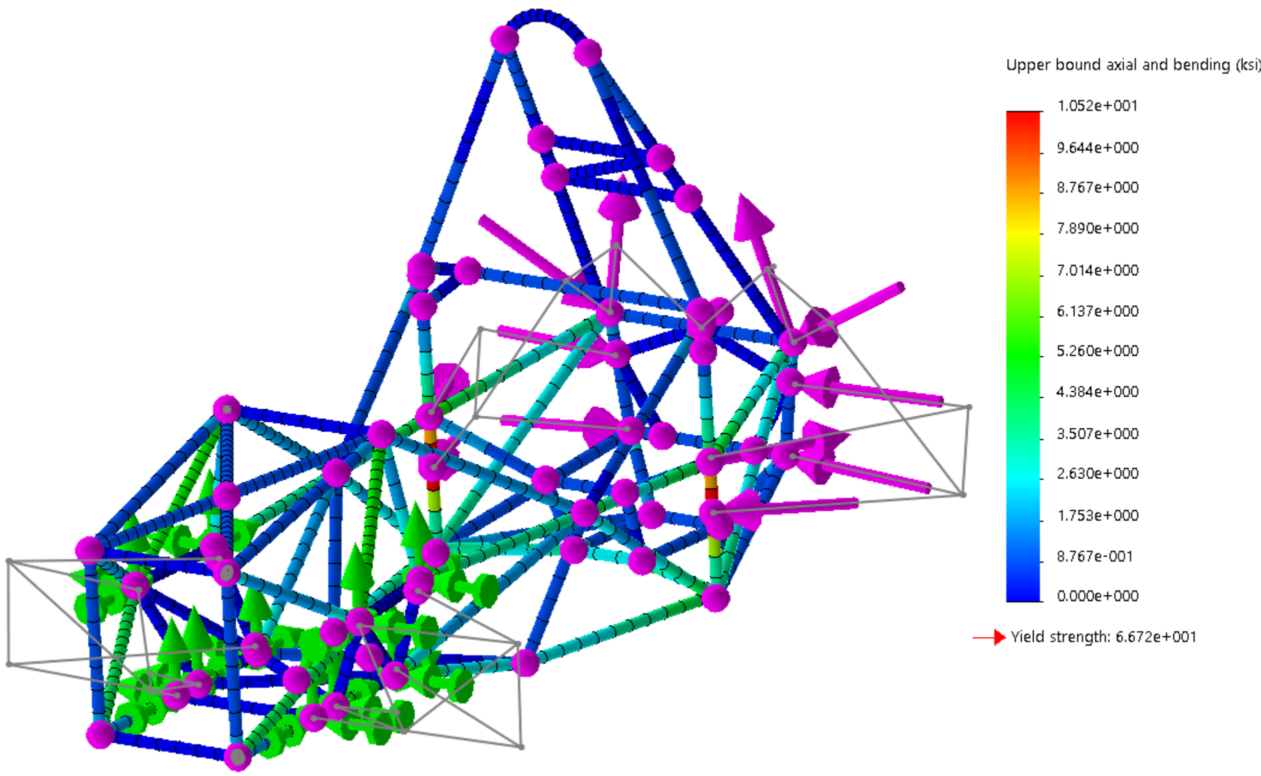

Figure 8: Stress on Rear Points Under 2.2G Braking

2.3 Deflection Under 1.8G Cornering

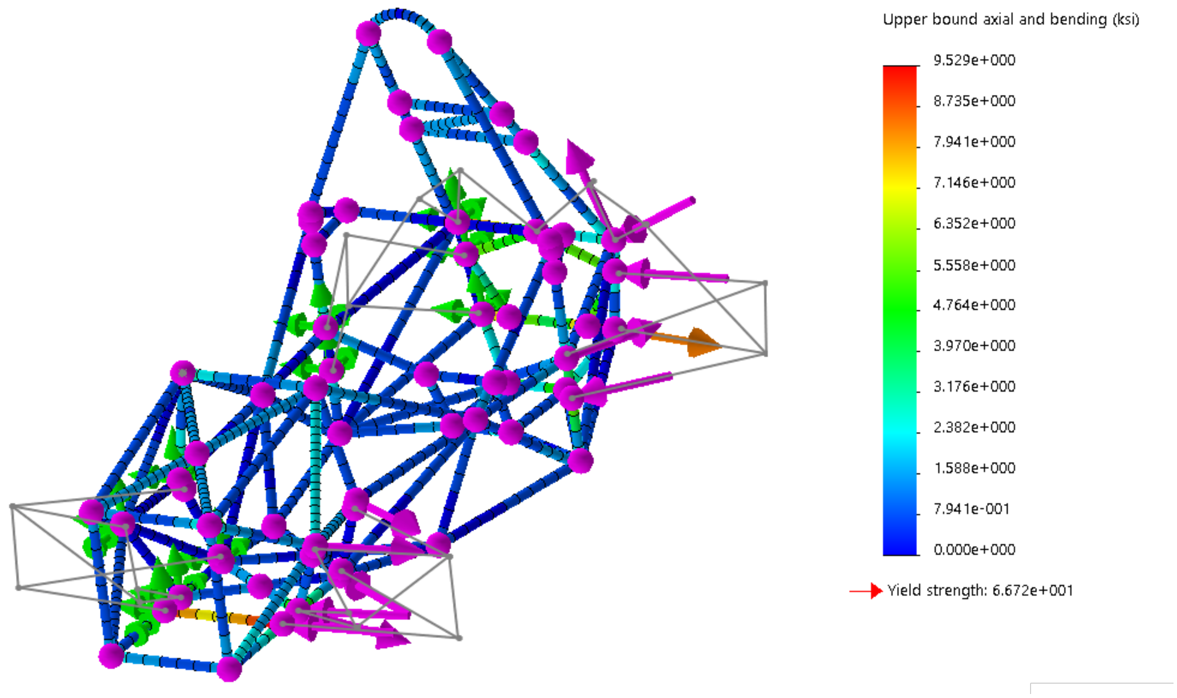

Figure 9: Stress on Inboard Points Under 2G Cornering

Suspension	Load Case	Camber Compliance (deg/G)
Front	2.2G Braking	.019
	2G Cornering	.008
Rear	2.2G Braking	.007
	2G Cornering	.008

Table 1: Camber and Toe Compliances for Front and Rear Suspension Nodes

2.4 Untriangulated Pickup Points

3 Engine Bay + Engine Mount Design

3.1 Goals

- Reduce weight of engine bay and rear bulkhead by a combined 0.5 lbs
- Achieve a factor of safety of 2.5
  - The yield criterion for the engine bay was set as the endurance limit of normalized 4130

steel (49 ksi)

- Increase tool clearances on engine bolts to allow for quicker engine replacement

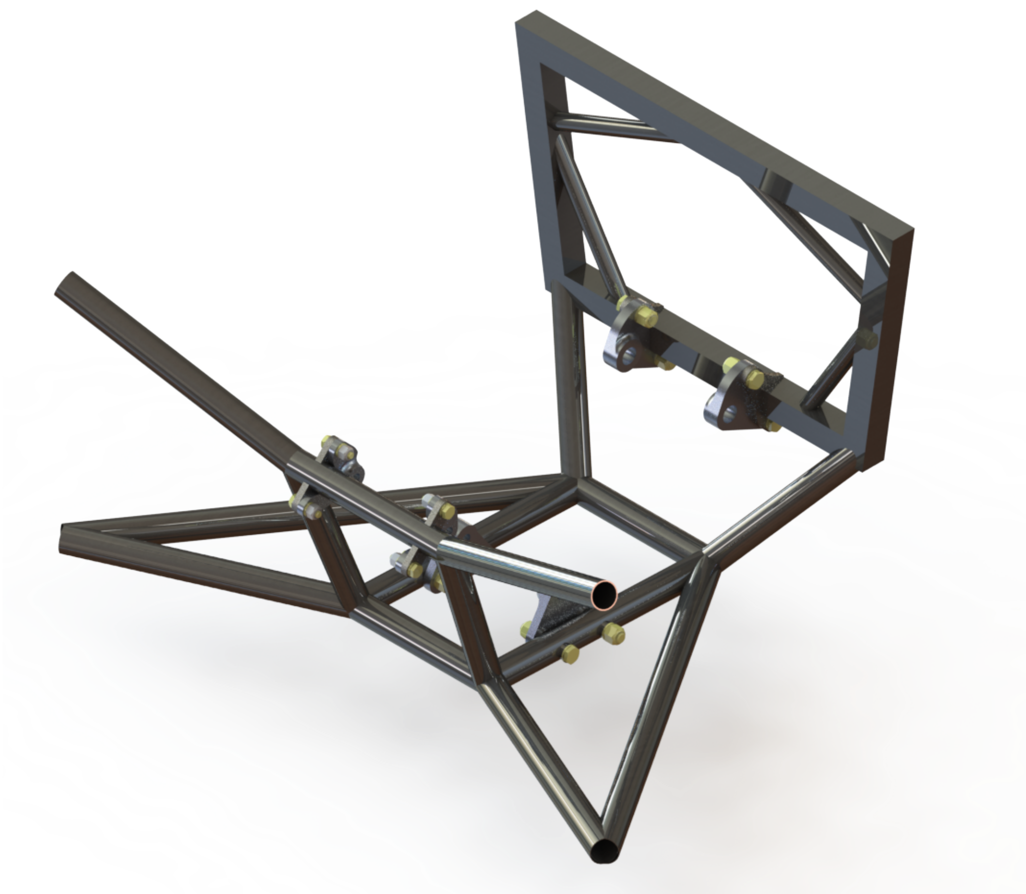

Figure 10: Final Engine Bay + Mount Design

3.2 Finite Element Model Setup

The FEA Model included simultaneous forces from

- Inertial Loading of Engine From Max Acceleration (34 lbf)
- Static Weight of Engine (52 lbf)
- Max Chain Line Load (2115 lbf)

with the engine modeled as 3/16 aluminum shell.

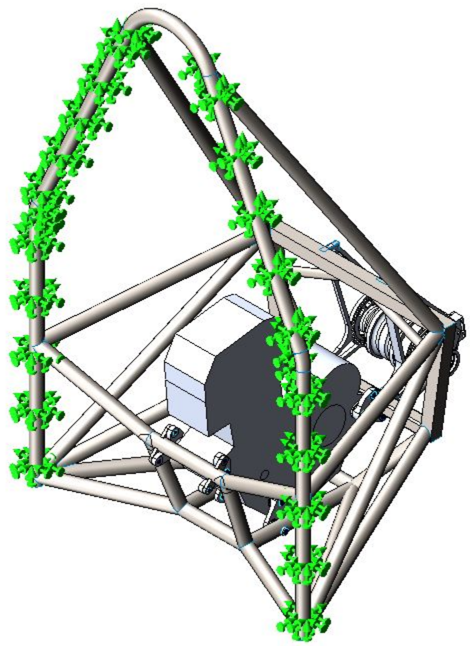

Figure 11: Engine Bay FEA Setup - Fixtures

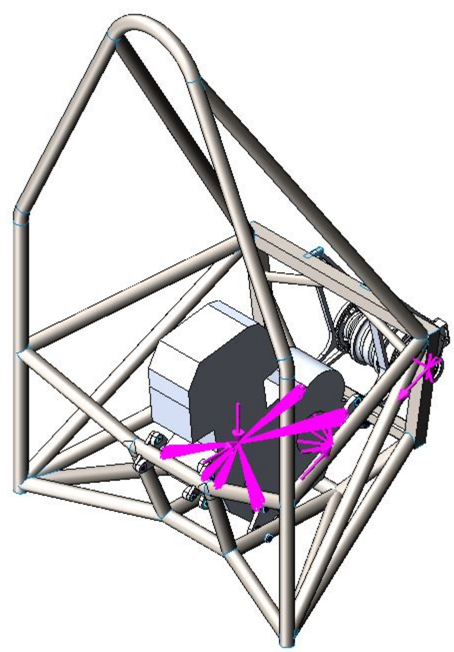

Figure 12: Engine Bay FEA Setup - Loads

3.3 FEA Results

Max stress was determined to be 20 ksi, giving a factor of safety of 2.45.

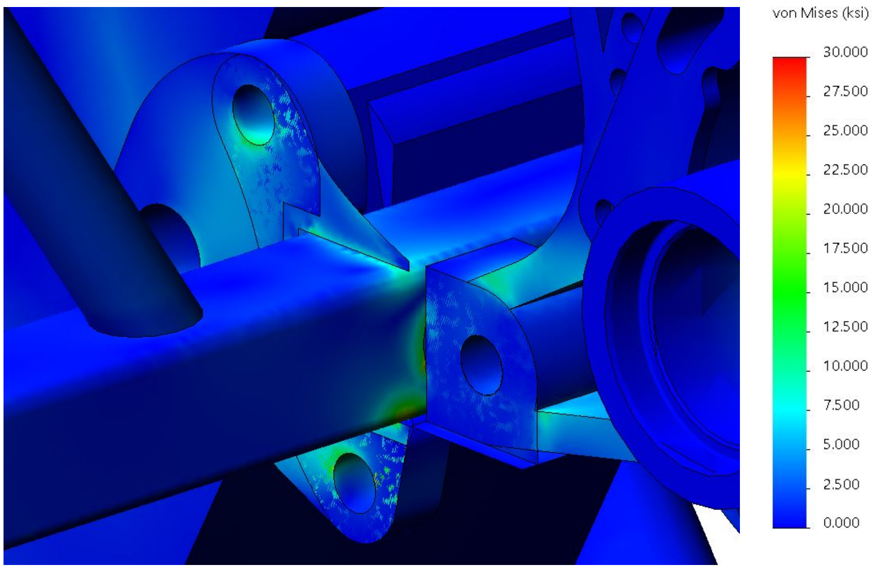

(a) Resultant Stress Distribution (b) Stress Scale

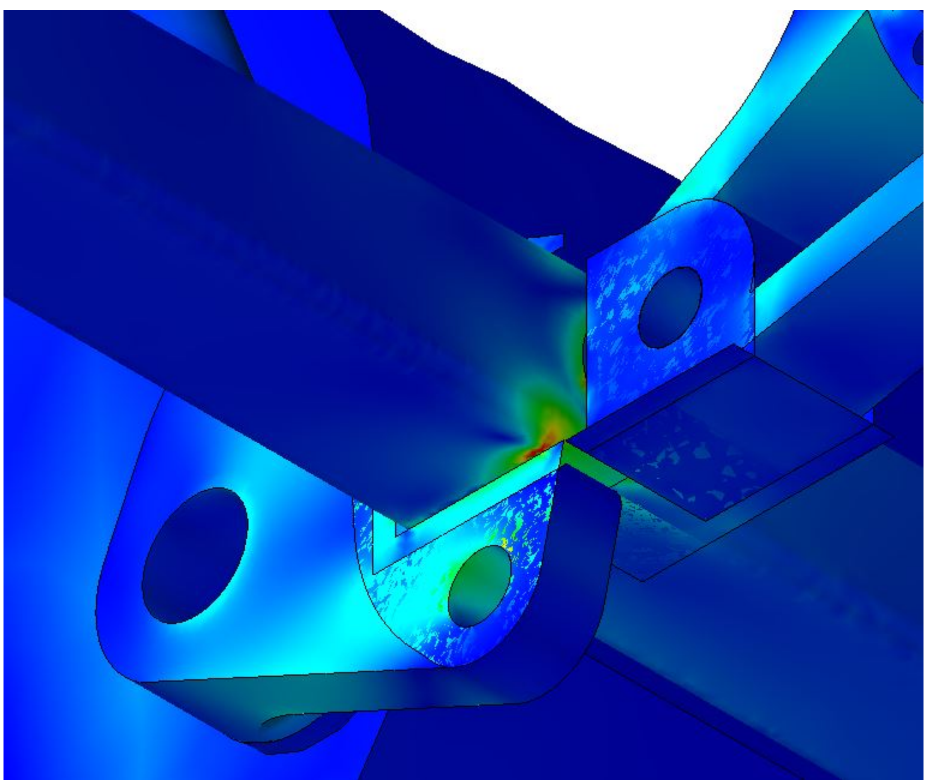

Figure 14: Resultant Stress Distribution

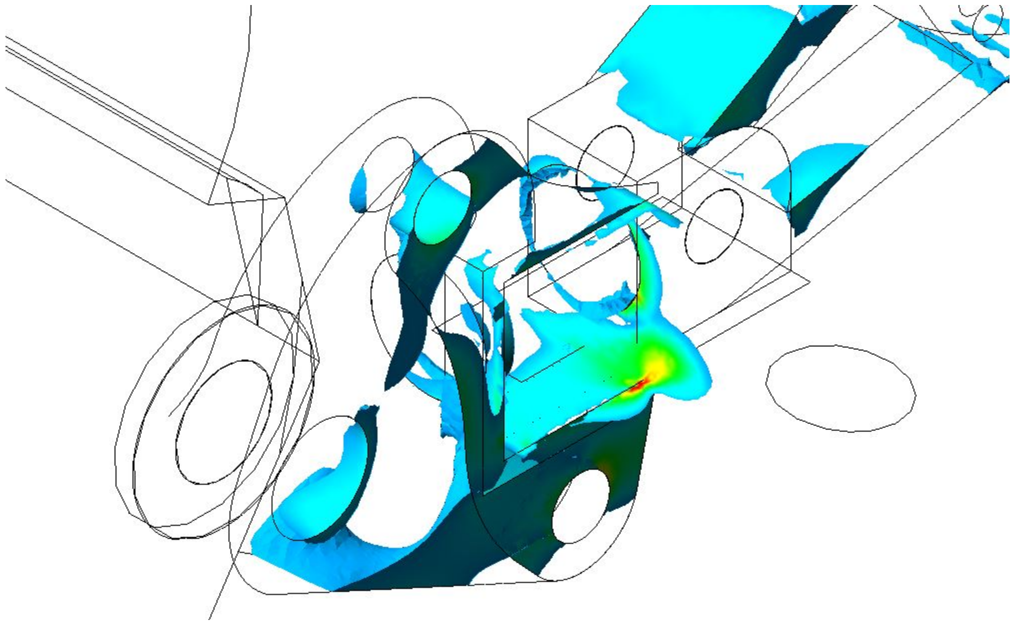

Figure 15: Iso-clipped at 5 ksi

Sidenote: Measured chainline load during testing turned out to be slightly lower at 1760 lbf in comparison to the target value of 2115 lbf. Max stress thereby dropped by 2.5 ksi to 17.5 ksi.

3.4 Engine Mounts

- The engine mounts consist of 7075-T6 aluminum mounts that are bolted to welded 4130 steel mounts
  - Designed in part to allow the team to swap engine models for testing
  - Size of the engine mounts was also increased this year to allow for better tool clearances and therefore faster engine removal and insertion
- In comparison to using only welded steel mounts, the aluminum + steel hybrid mounts result in an increase in only 0.42 lbs, including all hardware
  - The total weight of the engine mount system (excluding the bolts that go through the engine itself) is 2.27 lbs
- Engine mounts were designed to the endurance life of 7075-T6 aluminum (23 ksi) with a factor of safety of 1.75

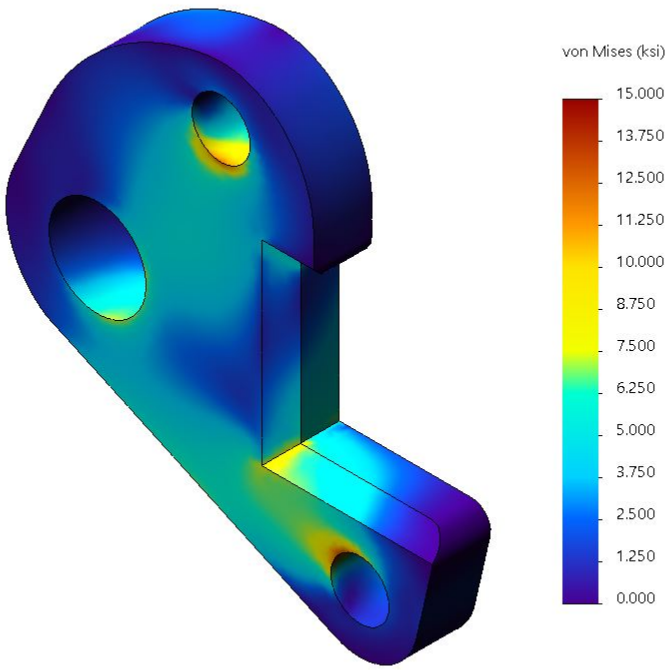

Figure 16: Rear Engine Mount Stress Distribution

The max stress on the rear engine mount was 13.3 ksi, giving a factor of safety of 1.73. The max stress on the front and lower mounts was significantly lower, and was in the range of 2 ksi.

Figure 17: Engine Mount Render

4 Modal Analysis

4.1 FEA Setup

- The model includes the suspension and uprights
- All suspension members are modeled with mass, stiffness, and end conditions identical to reality
- The engine is modeled as a rigid connection to the tubes where it mounts. This is appropriate because its specific mass and stiffness is far greater compared to the surrounding structure.
- The system is assumed to be free-floating on dampers. This makes it easy to validate, as the tires act as the dampers in a real-world test.

4.2 FEA Analysis

- The system was analyzed up to 200Hz (13000 rpm is the max engine frequency we see)
- The frequencies of the 4 main modes the system sees: 63 Hz, 85 Hz, 107 Hz, 128Hz
- The first two are torsion modes, with the third being a bending mode, while the fourth is general oscillation. This concurs with our assumption that the chassis is significantly stronger in bending than torsion
- In all cases the engine bay tubes move very little, if at all.

4.3 Verification

- We applied a moment to the chassis, torquing it
- The damping ratio we found is 0.084, with 95 confidence interval between 0.064 - 0.103.

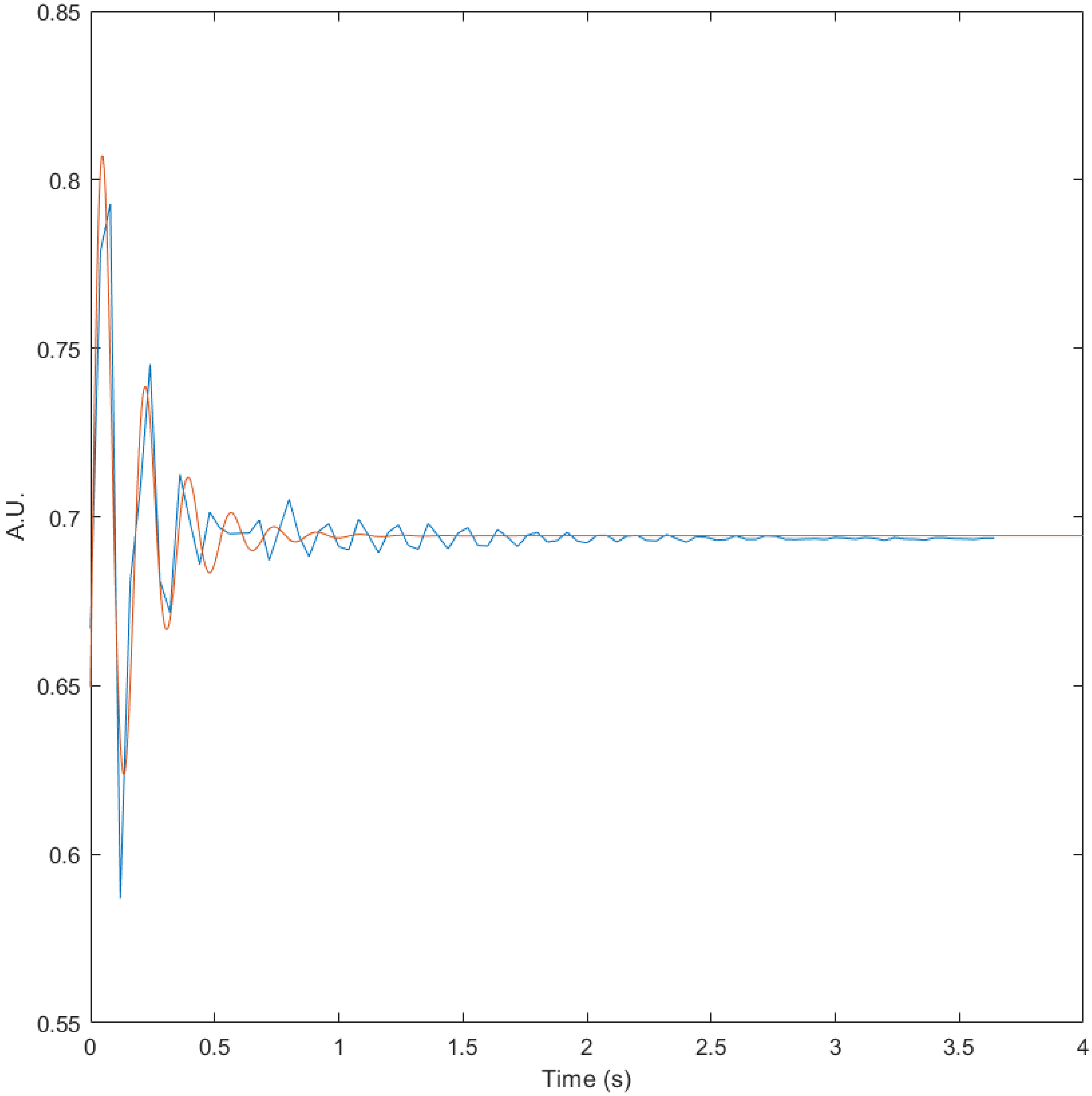

Figure 18: Curve fit of the dynamic response of the chassis in torsion

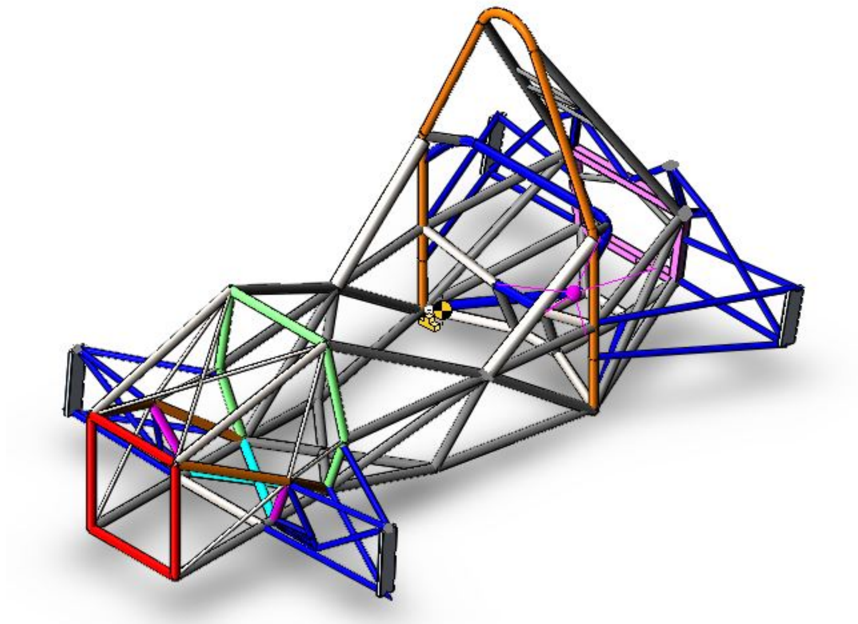

Figure 19: FEA Setup

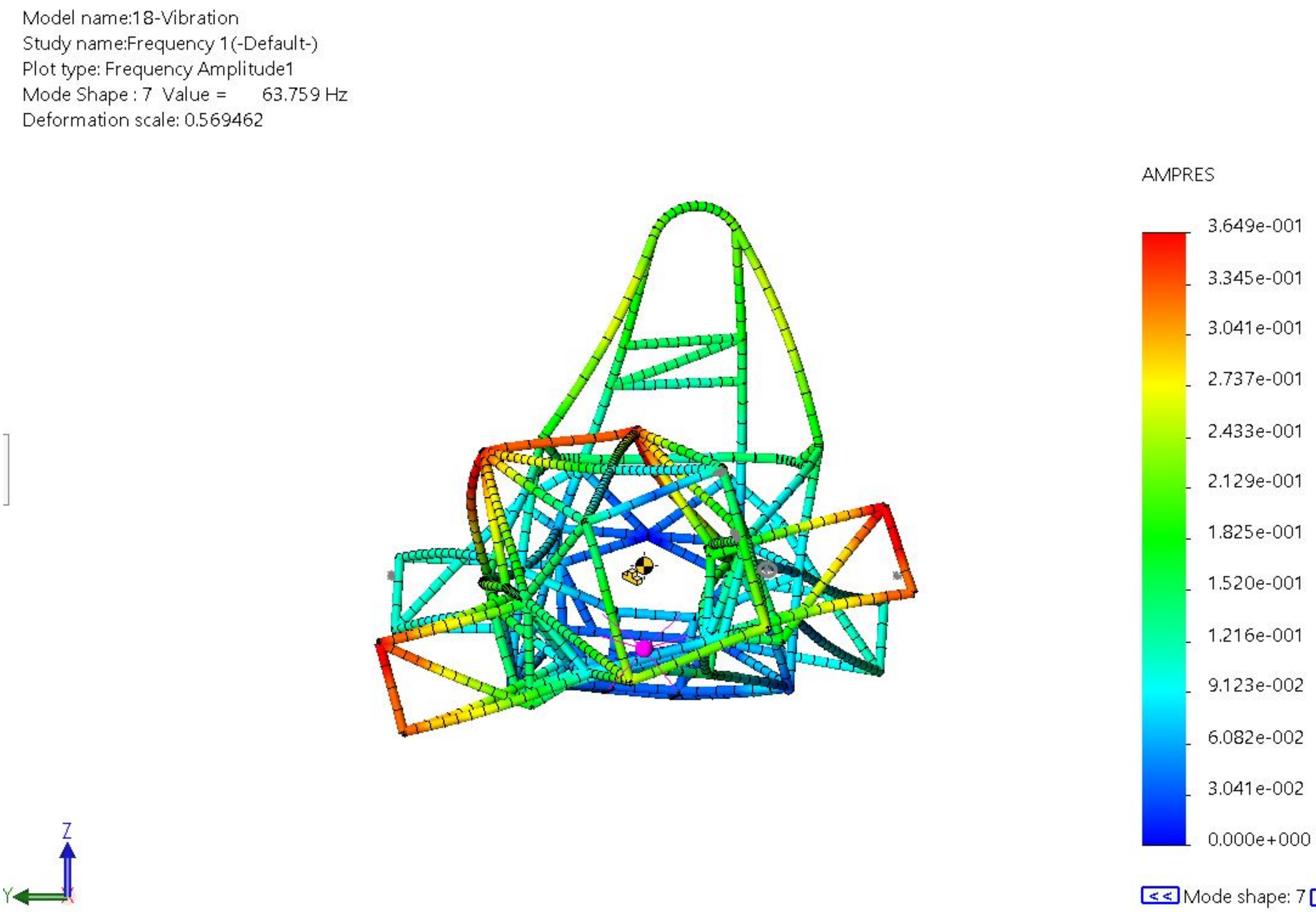

Figure 20: Resonant Frequency = 63hz, Torsional Mode

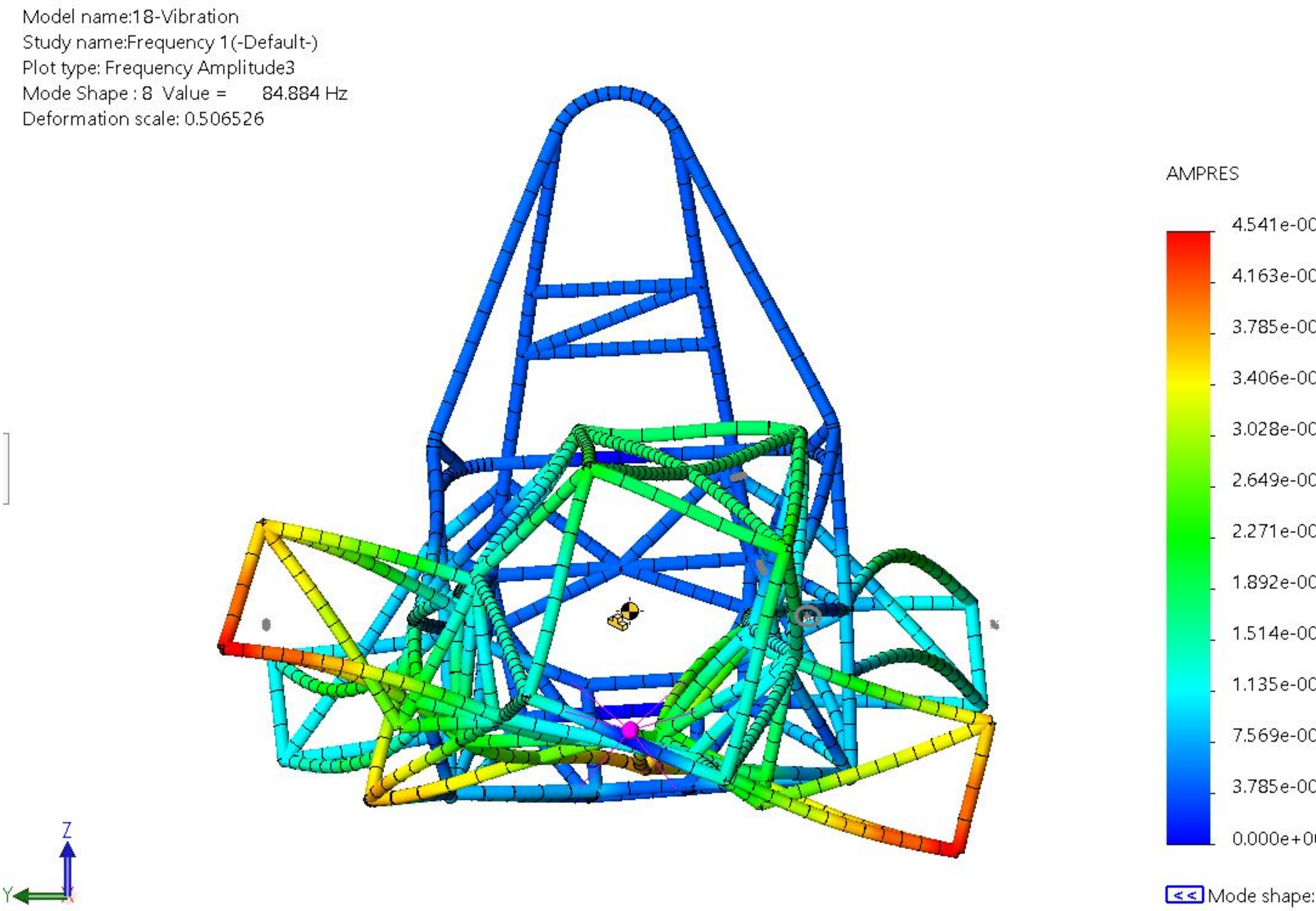

Figure 21: Resonant Frequency = 84hz, Torsional Mode

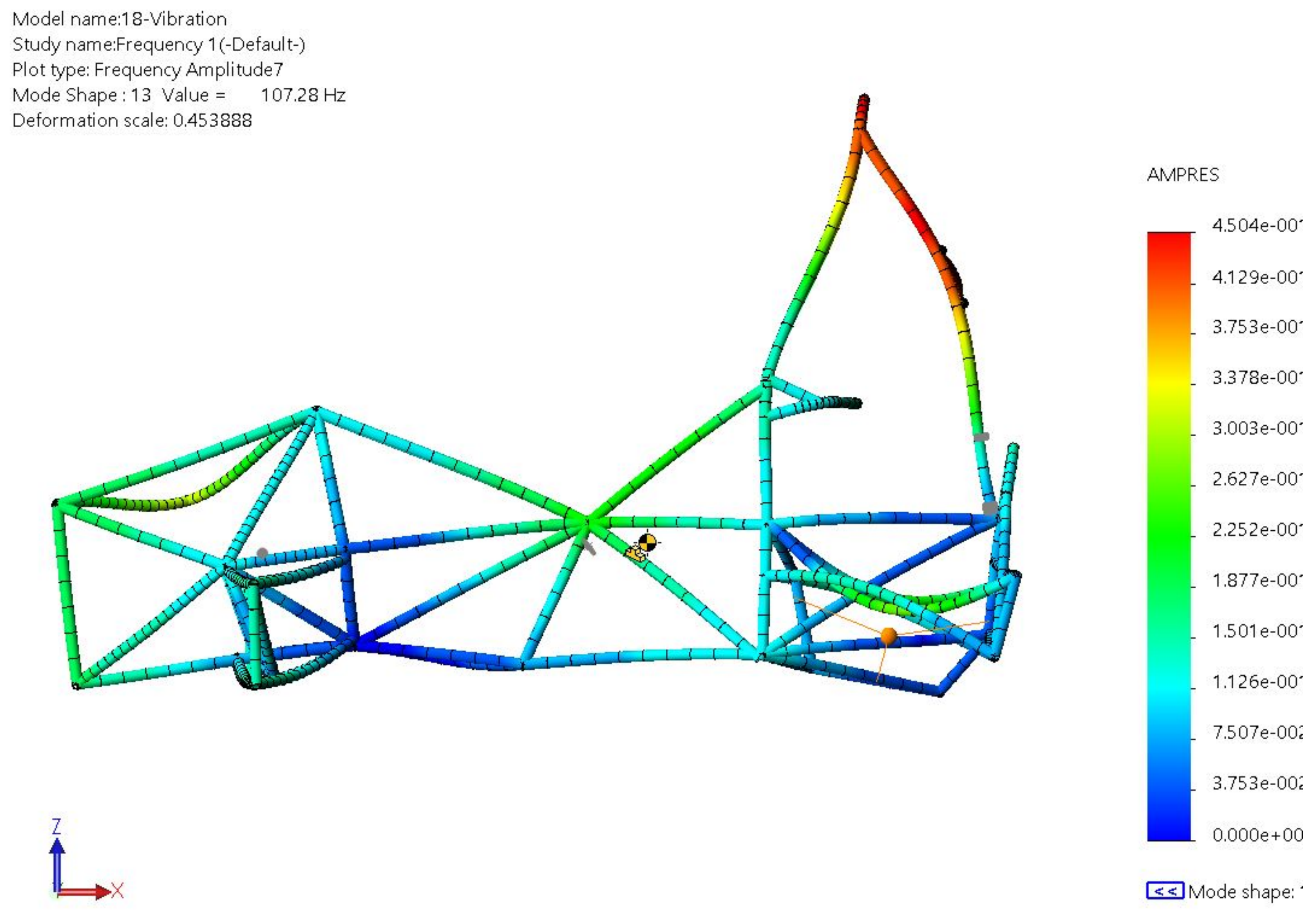

Figure 22: Resonant Frequency = hz, Bending Mode

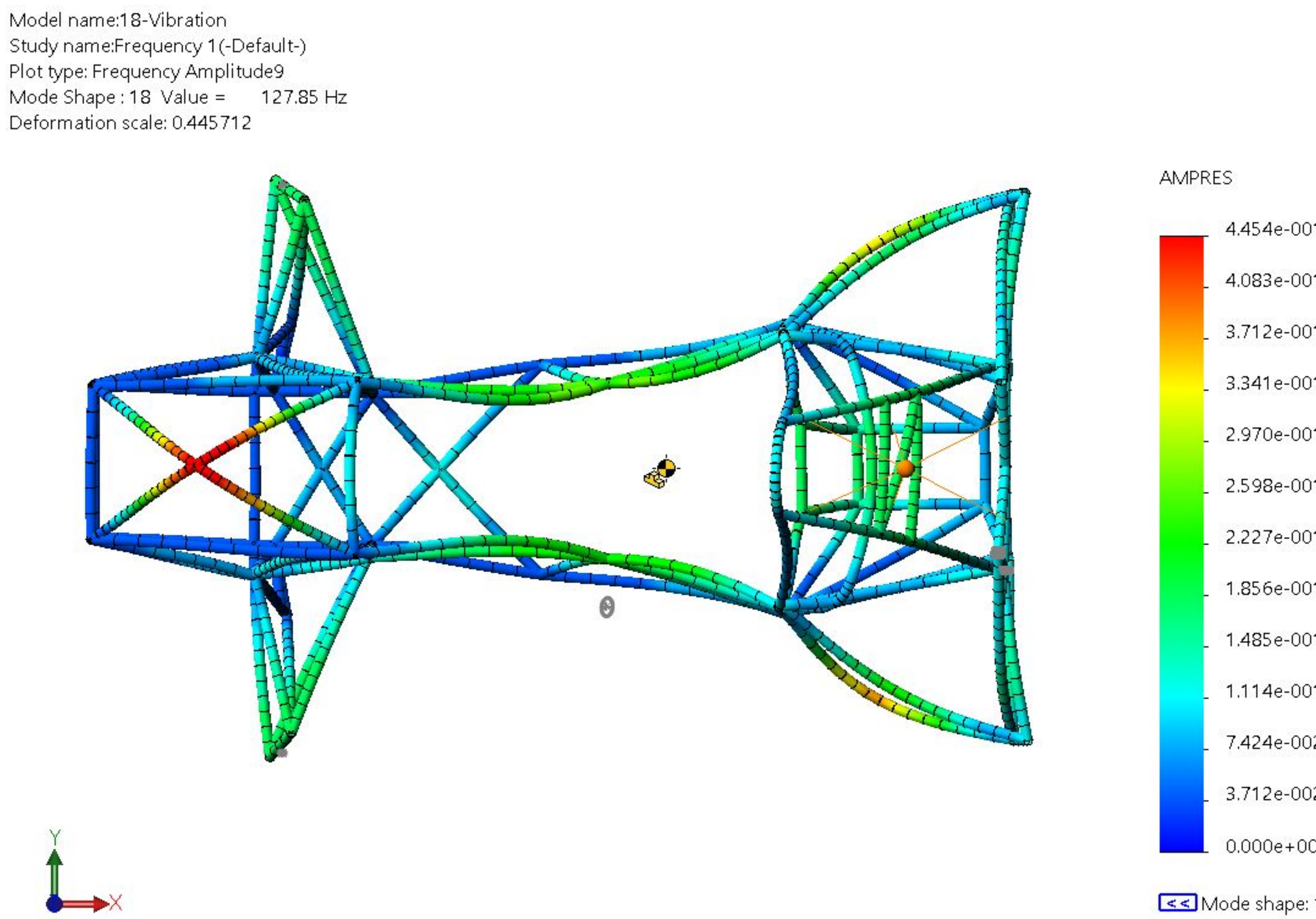

Figure 23: Resonant Frequency = hz, Bending Mode

5 Manufacturing

5.1 80-20 Jig

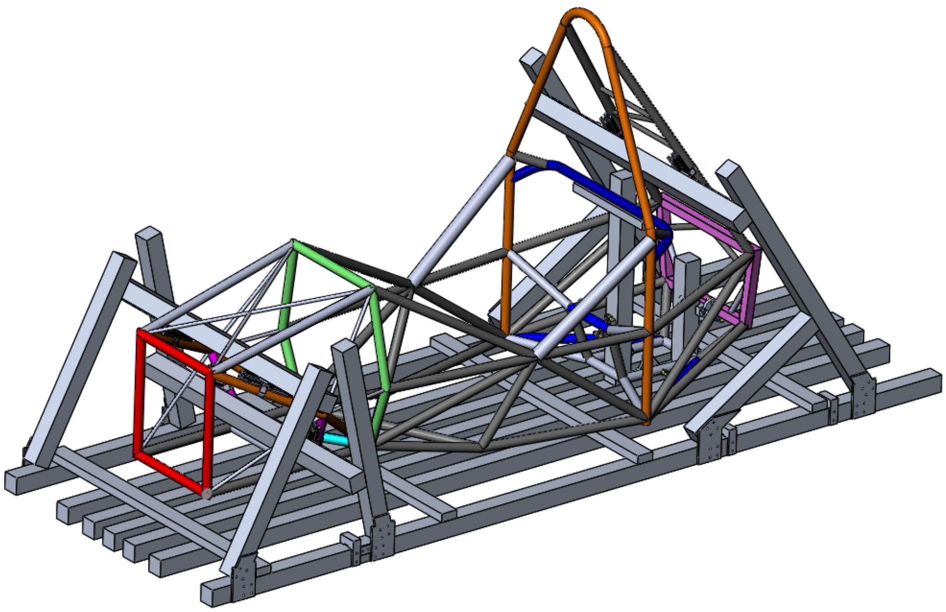

Figure 24: CAD Model of Chassis Welding Jig

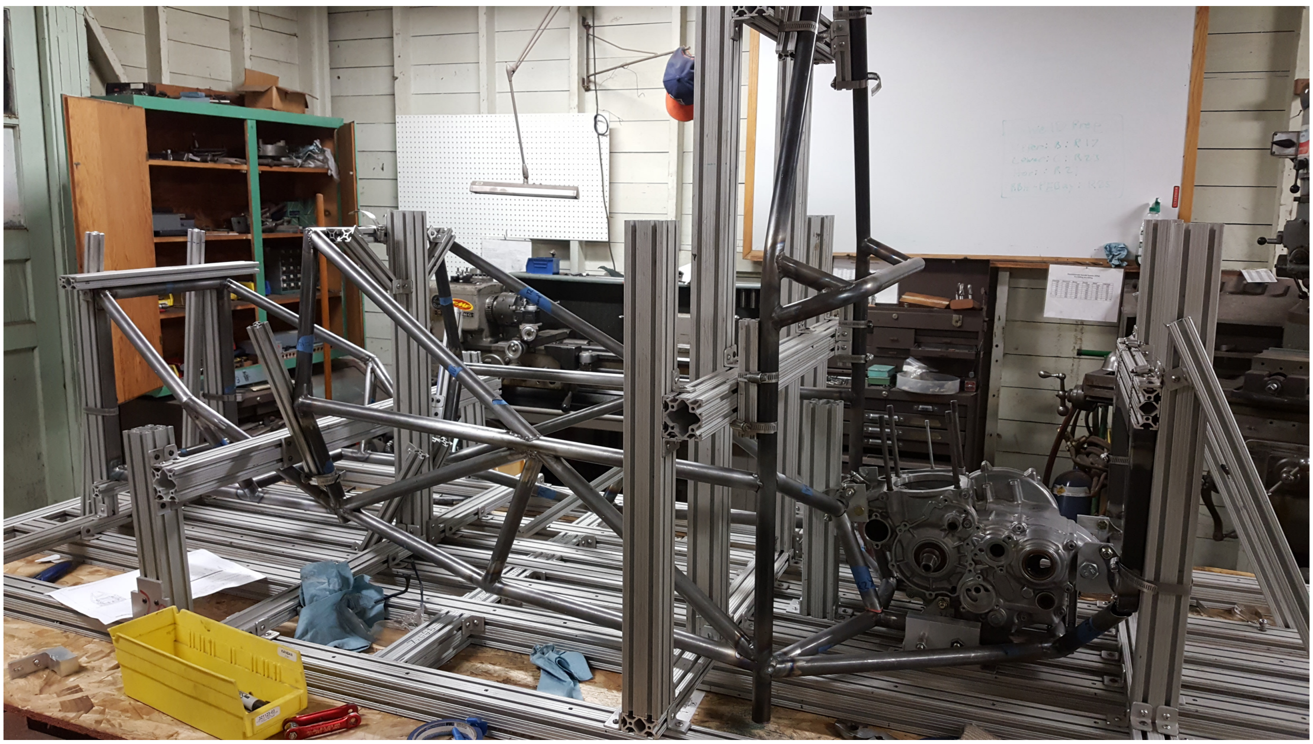

Figure 25: Side View of Chassis Welding Jig

5.2 Planar Jig

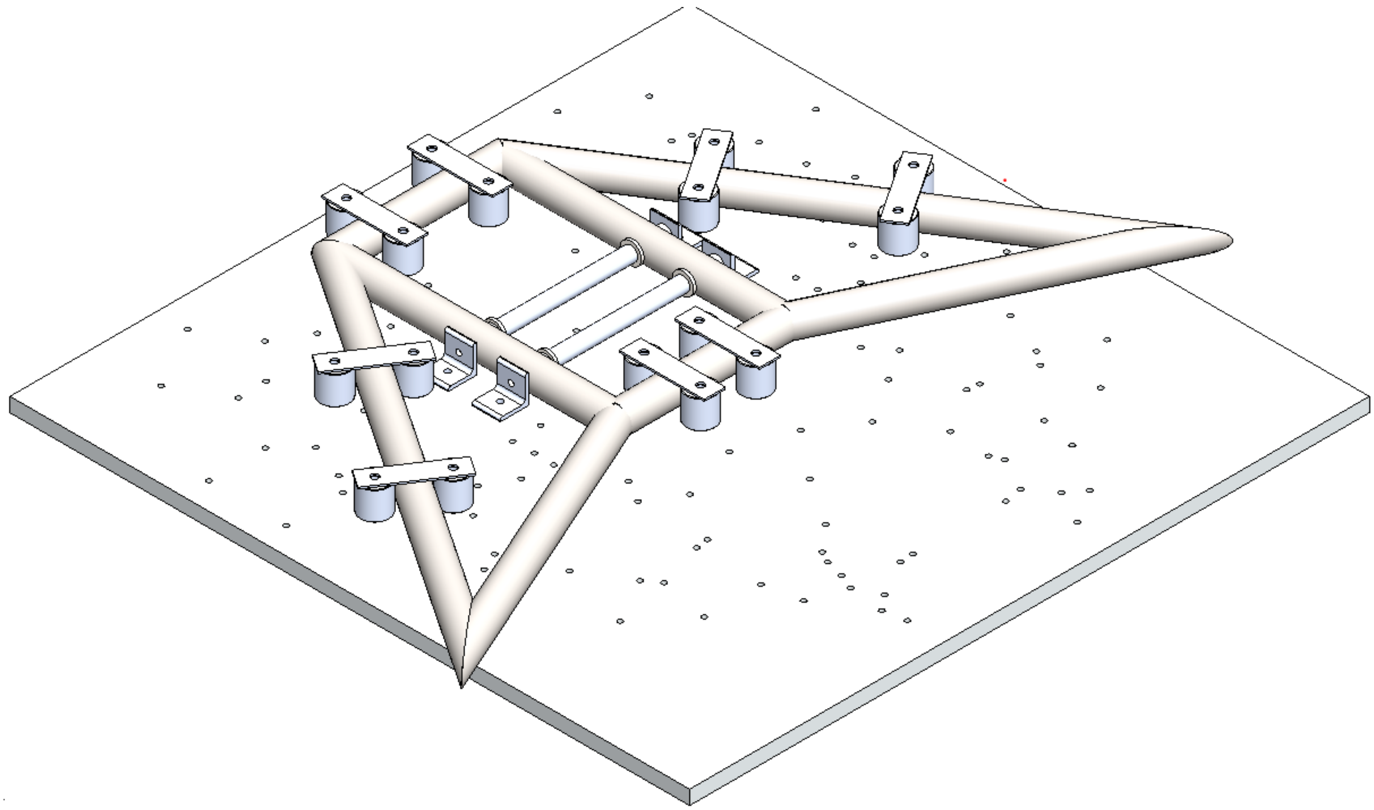

Figure 26: CAD Model of Planar Jig for Planar Section of Engine Bay

5.3 Suspension Jig

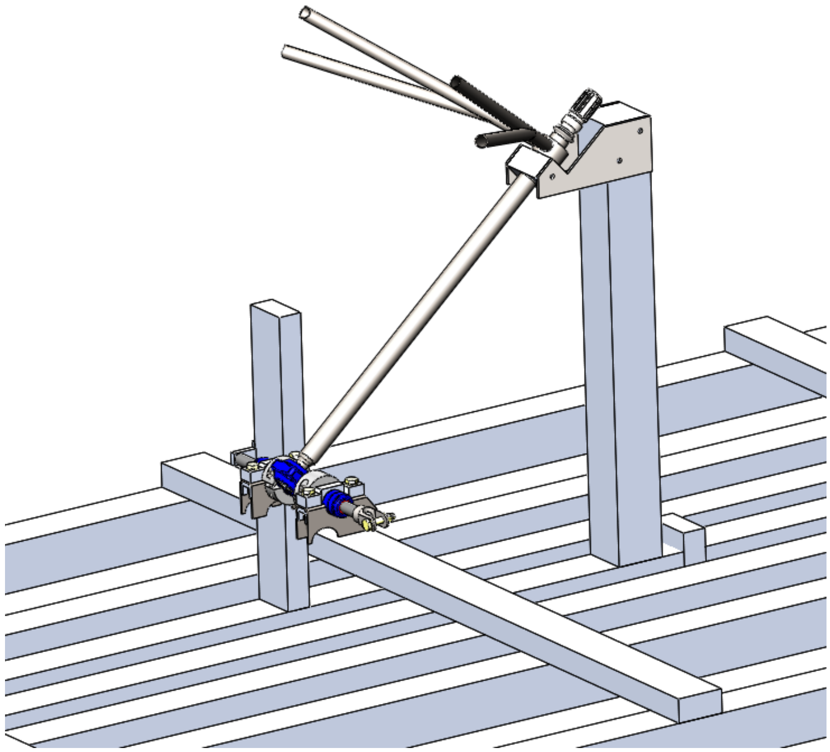

Figure 27: CAD Model of Steering Jig

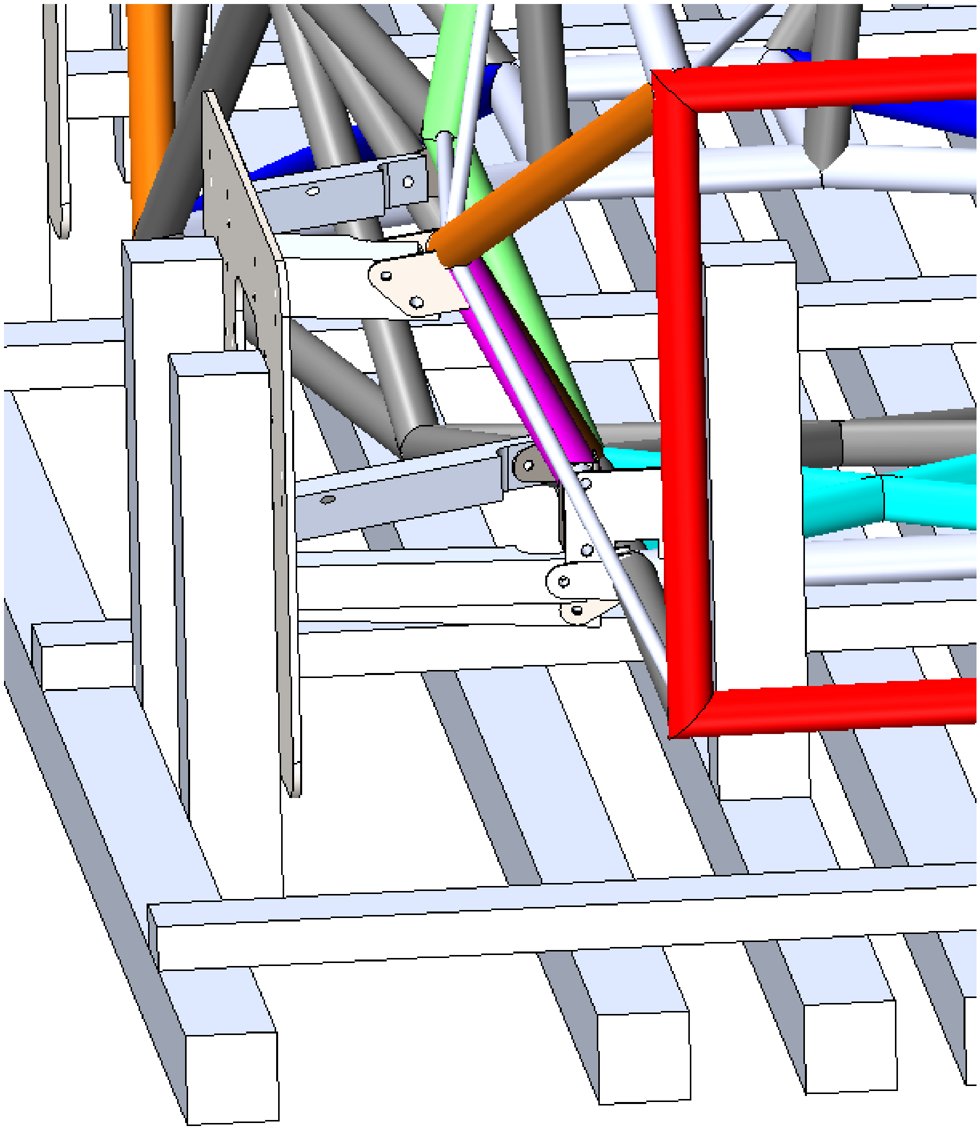

Figure 28: CAD Model of Front A-Arm Jig

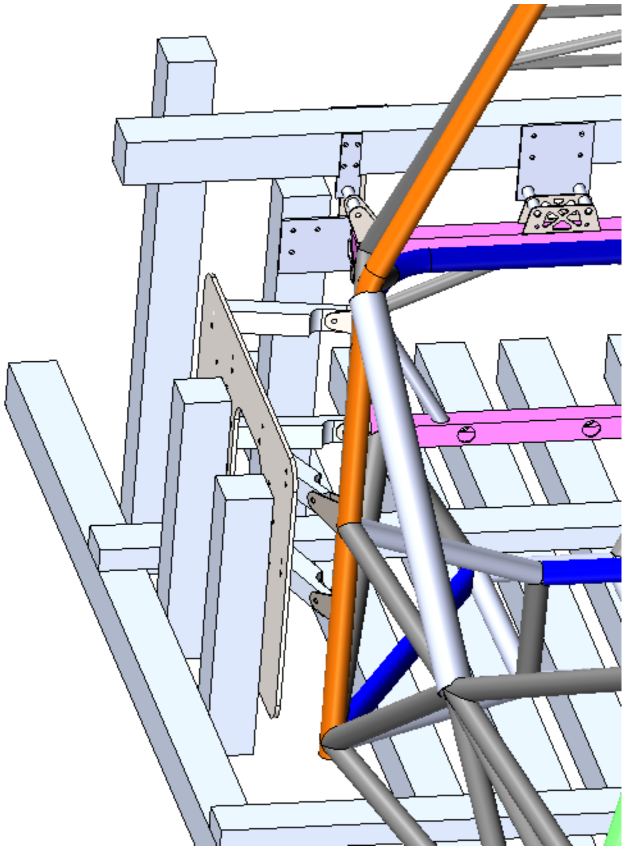

Figure 29: CAD Model of Rear A-Arm Jig

6 Research

6.1 Metal Normalization Investigation

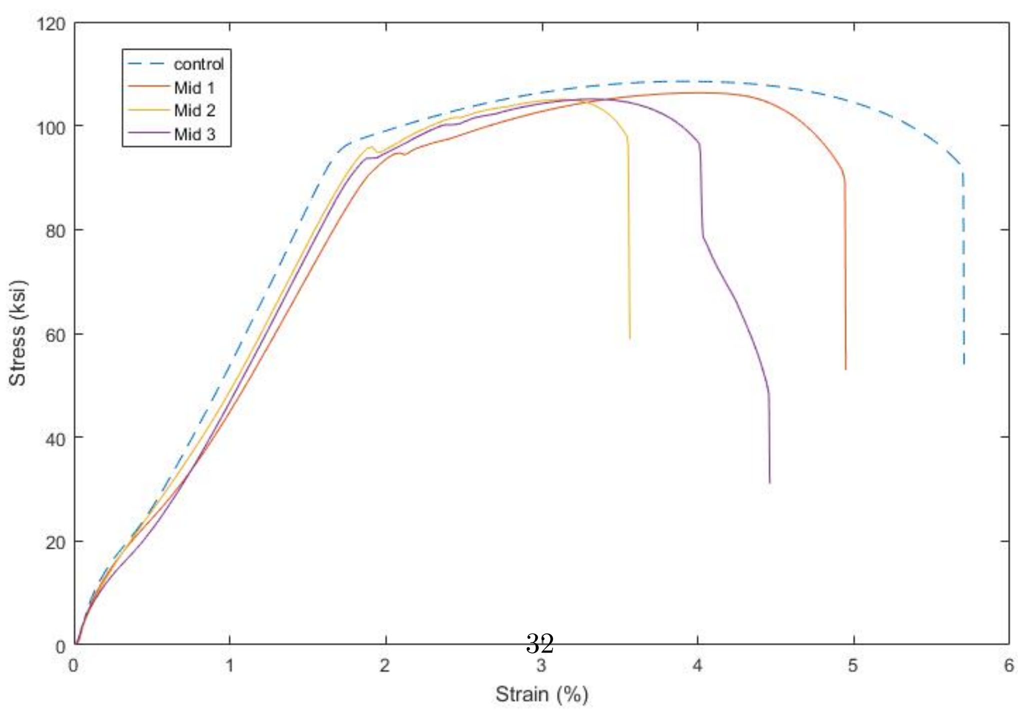

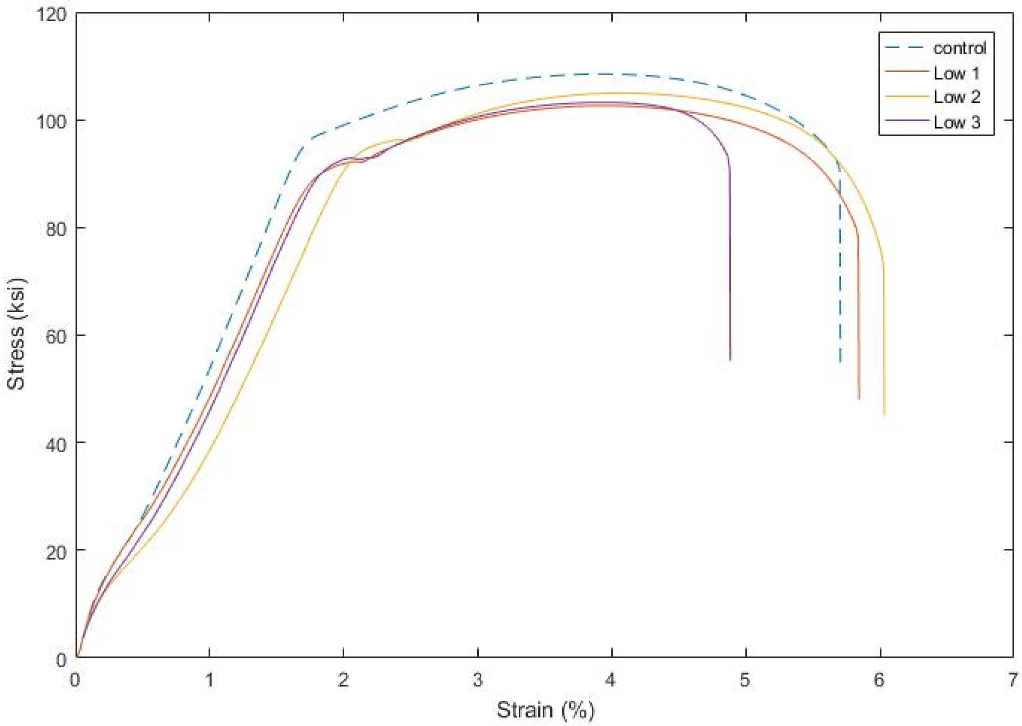

Figure 31: Stress Strain Curve for V tube Structure

6.2 Wishbone Analysis

Preliminary testing was performed in order to identify where failures would occur in welded specimens under tension and analyze the effects of welding within the heat affected zone. Three groups of three 4130 steel wishbone specimen having a thickness of 0.065" were loaded in tension until fracture on an Instron Tensile Machine. Group one is the control group that consists of water-jetted wishbones. Group two was welded a small distance below the mid-line of the specimen and group three was welded at the mid-line of the specimen. Stress-Strain curves for each of the 9 samples are obtained and presented in the figures below.

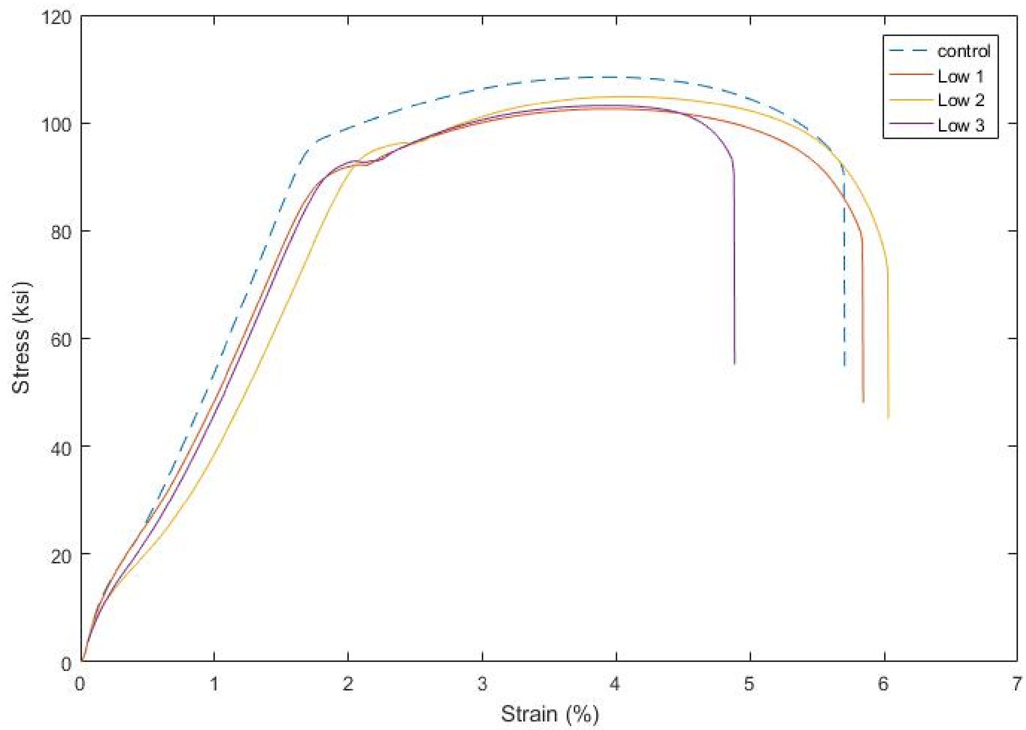

Figure 32: Control vs Lower Weld Stress-Strain Curve

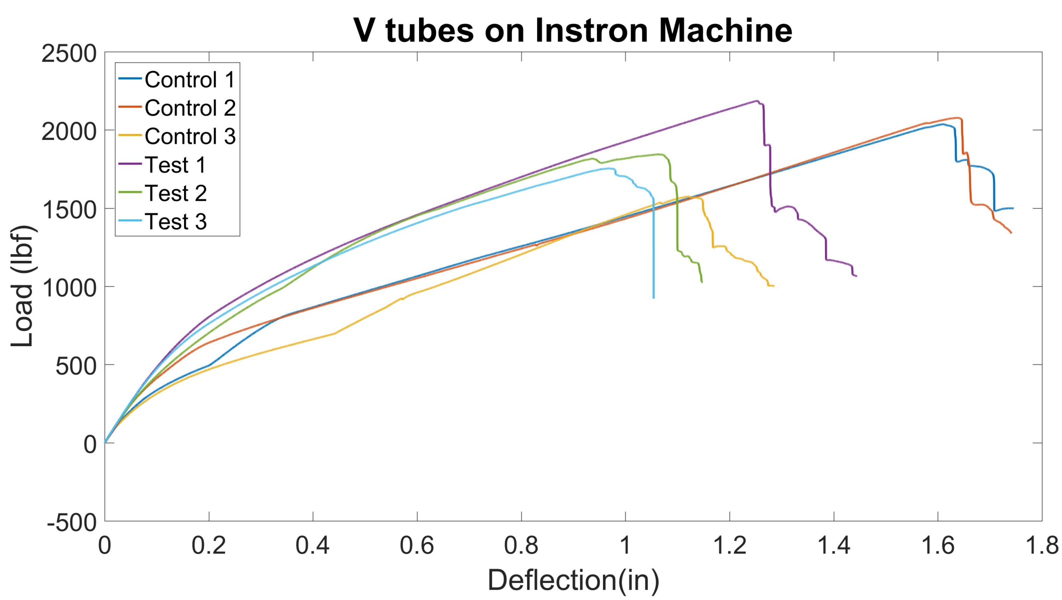

Figure 33: Control vs Lower Weld Stress-Strain Curve

Trial	Yield Strength (ksi)	True Ultimate Strength (Engineering) (ksi)	Ductility (Percent)	Toughness ($\frac{J}{m^3}$)
Control	95	113 (109)	5.73	8,692
Lower Weld	93	107 (103.5)	5.58	7,866
Mid Weld	89	109 (105.5)	4.18	5,770

Table 2: Weld Strength Comparison

Figure 34: Fractured Specimens and Fracture Locations

As seen in the image above, the welded specimens fractured at the edges of the heat affected zone, where residual stress is likely concentrated due to large temperature difference. Group 3 underwent multiple weld beads. The heat from the extra weld beads made group 3 more brittle and more susceptible to fracture, with a 1.55 percent reduction of ductility from the control group. Our third finding is that the surround material of a weld is more likely to fail or fracture than the weld itself.

6.3 Sandwich Panel Testing

- Sandwich panels were subjected to 3 point bend and punch shear tests.
- Why? Calculate the energy absorbed in the event of an impact and the perimeter shear maximum in the event of a pierce of the carbon fiber laminate panel.
- Purpose? To determine whether our available materials and manufacturing processes meet the rules requirements for composite strength and toughness